Chapter III.9

Accelerator driven systems

Frédéric Bouly
Laboratory of Subatomic Physics and Cosmology (LPSC), Grenoble, France

Accelerator driven systems (ADS) are considered as devices for the transmutation of long-lived nuclear waste. This chapter aims at giving an overview of the nuclear waste management issues and the accelerator requirements for successful ADS operation, in particular the stringent beam availability requirement. It then highlights the most significant activities worldwide in this domain. Common features are: high-power superconducting proton linacs and reliability-oriented R&D.

III.9.1 Introduction and historical context

An Accelerator Driven System (ADS) is a nuclear reactor driven by a proton accelerator that allows the continuous injection of neutrons to maintain nuclear power production in a subcritical environment.This hybrid system is nowadays commonly considered as a possible device for nuclear waste incineration; in particular long-lived minor actinides that are produced in nuclear reactors. In its most general form, an ADS is composed of three main elements (see Fig. III.9.1):

- A subcritical reactor, inside which the nuclear waste to be incinerated, or transmuted, is introduced with the fuel;
- A heavy-material target which, when hit by protons, generates a flux of neutrons through the spallation process;
- A high-energy and high-power proton accelerator.

Historically, particle accelerators have been considered for the production of fissile materials. Indeed, industrial-scale applications started in 1950, when E. O. Lawrence launched the Materials Testing Accelerator (MTA) project at the Lawrence Livermore National Laboratory [1], in particular to produce ^{239}Pu. Before the 1960s, the aim was to get the most out of uranium by transforming it into ^{239}Pu by neutron irradiation. This was done either in breeder reactors (but they needed fissile material to start up), or with accelerators that needed electricity to operate. Consequently, the use of particle accelerators appeared to be a method of producing fissile material from available electricity. The main aim was to produce plutonium for military purposes.
At a later stage, W. B. Lewis also proposed using an accelerator to breed ^{233}U fuel from natural thorium for CANDU reactors (Canada) [2]. Nevertheless, in the 1960s, uranium-rich deposits were discovered

This chapter should be cited as: Accelerator Driven Systems, F. Bouly, DOI: 10.23730/CYRSP-2024-003.2085, in: Proceedings of the Joint Universities Accelerator School (JUAS): Courses and exercises, E. Métral (ed.),
CERN Yellow Reports: School Proceedings, CERN-2024-003, DOI: 10.23730/CYRSP-2024-003, p. 2085.

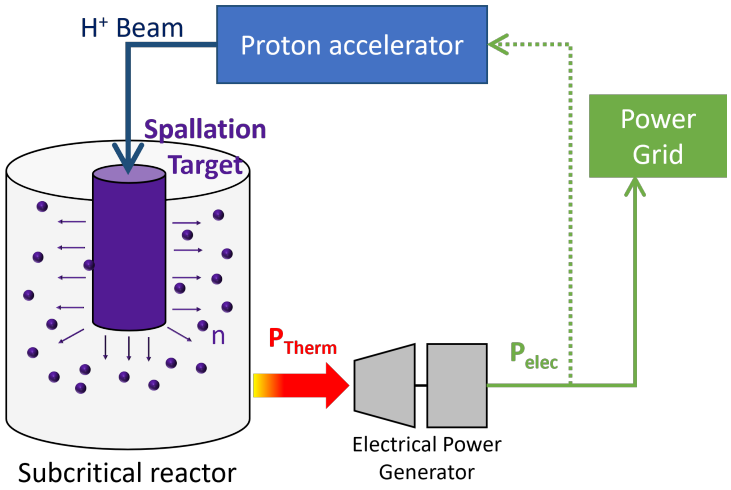

Fig. III.9.1: ADS principle.

in the United States and these projects were slowed down. Indeed it was also realised that a beam power of several hundred MW would be required for these methods to be practical [3].

Motivated by the significant developments of accelerator technology since the 1950s, the idea of coupling an accelerator to a reactor, so that the latter benefits directly from the neutrons produced by the former, was proposed towards the end of the 1970s : in particular at Brookhaven, with the PHOENIX concept [4]. Its purpose was to transmute nuclear waste with a fast-neutron ADS and a high neutron multiplication factor. In such an approach, the continuous injection of neutrons enables to generate subcritical neutron chains, characterised by a neutron multiplication coefficient $k_{\text{eff}} < 1$.

All these projects, developed mainly in the United States during the 1970s, were mostly motivated by the desire to develop proliferation-resistant nuclear systems (following the non-proliferation policy introduced by the Carter administration in 1976). Today, the focus has shifted to the transmutation of long-lived waste, reflecting new environmental and energy concerns. Many ADS projects arose in the 1980s and 1990s (for example OMEGA in Japan [5]) and more details are given in Ref. [3] on these projects.
Among them, one could highlight the CERN "Energy Amplifier" ADS concept [6], developed by C. Rubbia which claimed that the energy provided by the proton beam could be "amplified" through fission reactions in the system's core (principle of Fig. III.9.1). This work triggered the actual ADS R&D in Europe, and in the entire world, that essentially aims at demonstrating the feasibility of high-power ADS operation to incinerate long-lived nuclear waste.

III.9.2 Nuclear waste management issues

Since the early 1930s, with the discovery of the fission phenomenon, technologies using nuclear energy have undergone considerable development, in particular for electricity generation. The fission reactions of atomic nuclei such as uranium 235 or plutonium 239, currently used in nuclear power reactors, are extremely calorific and do not directly release carbon dioxide. As an order of magnitude, the electrical energy that could be produced with the fission of 1 g of ^{235}U would be equivalent to the combustion of $\sim$ 1.2 t of oil or $\sim$1.7 t of coal[1].

Nuclear energy is also attractive in terms of cost and was particularly developed during the oil crisis of the 1970s. In Europe, about 143 nuclear units supply more than 20 % of the electricity generated on the continent [8], as illustrated in Fig. III.9.2, even if one could observe a slight decrease of nuclear power for electricity production since 2010. Still, the use of nuclear power may fluctuate according to geopolitical situation in Europe, as well as the use of coal and natural gas. Renewable energies production is growing, but seems to be not mature enough, or sufficiently developed, to supply the demand. Nuclear plants appear to be the preferred solution in several countries to mitigate the energy transition within the coming decades.

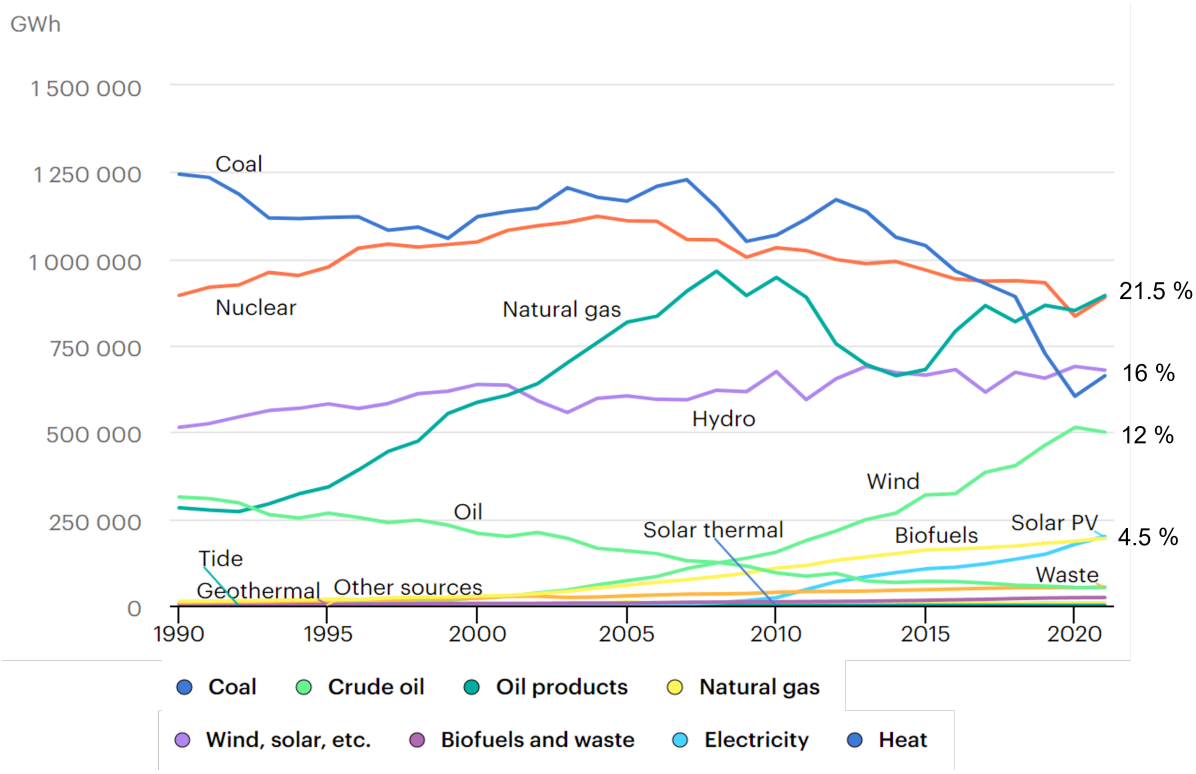

Fig. III.9.2: Electricity generation by source, in Europe (1990–2021) [8].

However, even if some of the spent fuel is recycled, nuclear activity generates highly radioactive waste. Yet, waste contains radio-toxic substances with decay periods well beyond those experienced by human societies. Their accumulation raise societal, political and safety issues. It is therefore crucial

[1]Considering 1 g of pure ^{235}U and that the energy generated per fission is $\sim$ 200 MeV. The considered calorific value for oil is 42 GJ/t, and 29.3 GJ/t for coal [7]. The considered efficiency, to convert thermal energy into electrical energy, is $\sim$ 33 % for a nuclear power plant and $\sim$ 55 % for a combustion power plant.

to have reliable and sociologically acceptable technical solutions for managing this waste over the very long term and to limit their accumulation.

III.9.2.1 Present situation

The use of radionuclides in many sectors generate waste. This waste, in gaseous, liquid or solid form, can be toxic to humans and the environment. However, most of the radioactive waste (~ 65 %) comes from nuclear power generation. Nuclear waste is classified according to its specific activity level, generally expressed in becquerels per kilogram[2] (see Eq. III.9.3). They can also be characterised by their radioactive half-life.

The radioactive decay law states that the probability per unit time that a nucleus will decay is a constant, λ, independent of time. This constant probability may vary greatly between different types of nuclei. The decay law, giving the the total number N of radioactive nuclei remaining after time t is

$$N = N_0\, e^{-\lambda t}, \tag{III.9.1}$$

with N_0 the initial number of nuclei at $t = 0$.

Moreover, the half-life ($t_{1/2}$) of a nuclide is the time after which the amount of these nuclides is halved[3]. The relationship between λ and $t_{1/2}$ derived from the decay law is

$$t_{1/2} = \frac{\ln 2}{\lambda}. \tag{III.9.2}$$

And the nuclear activity, $A(t)$, is finally defined as

$$A(t) = \lambda N(t). \tag{III.9.3}$$

In Europe - following the recommendations made by IAEA (International Atomic Energy Agency) system - waste can be classified in five different categories [10]:

- Very low-level waste (VLLW);
- Short-lived (half-life of less than 31 years) low-level and intermediate-level waste (LLW and ILW);
- Transition waste (equivalent to short-lived LLW);
- Long-lived (half-life longer than 31 years) low-level and intermediate-level waste (LLW and ILW);
- High-level waste (HLW).

Around 2.5 million m^3 of low- and intermediate-level waste (VLLW, ILW and LLW short and long lived) has been generated in Europe [11]. VLLW are from the dismantling of nuclear facilities or from conventional industries using naturally radioactive materials. It generally takes the form of inert waste (concrete, rubble, etc.). Short-lived ILW and LLW are mainly related to maintenance (clothing,

[2] Activity represents the number of disintegration per second within a radioactive material; it is measured in becquerel (1 Bq = 1 desintegration/s) or curie (1 Ci $= 3,7.10^{10}$Bq).

[3] Generally, a distinction is made between waste whose main radionuclides have a short half-life (less than or equal to 31 years) and waste with a long half-life (greater than 31 years). It is considered that the radioactivity is greatly attenuated after 10 half-lives, i.e. $\sim$ 300 years for long-lived waste.

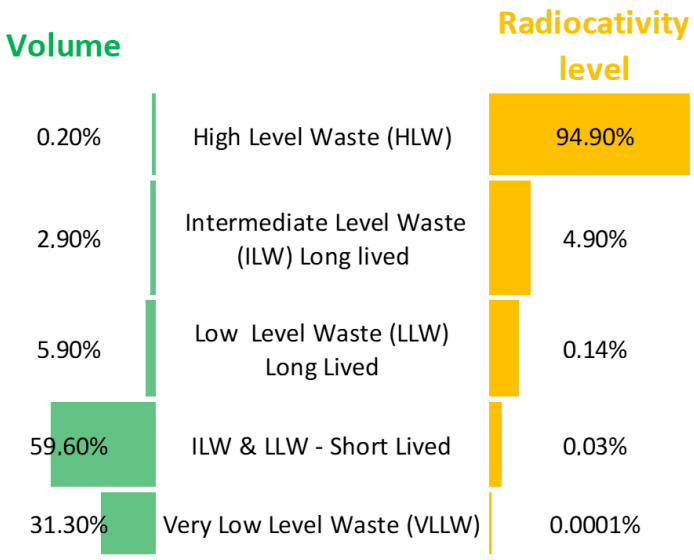

Fig. III.9.3: Classification of radioactive waste and distribution (in % of total volume), in 2020 (ANDRA, France) [9].

tools, filters, etc.) and to the operation of nuclear facilities (treatment of liquid effluents or filtration of gaseous effluents). They may also come from clean-up and dismantling operations. Long-lived LLW and ILW come mainly from the structures surrounding spent fuel and the products of ore processing for fuel fabrication.

Fig. III.9.3 represents the nuclear waste distribution in France, which illustrates the case of countries where uranium ore and plotunium from burnt fuel are reprocessed and therefore not considered as waste. The HLW are the final products generated directly from spent fuel. It only represents 0.2 % of nuclear waste, but almost 95% of the total radioactivity.

Depending on the adopted strategy for fuel reprocessing, the HLW inventory may vary from one country to another. Still, to give an order of magnitude, in 2019 ∼60 000 tons of spent nuclear fuel (HLW) were stored across Europe (excluding Russia and Slovakia) : ∼25 % in France, ∼15 % in th UK and ∼14 % in Germany [11]. This spent fuel is considered as HLW. Though present in comparably small volumes, it makes up the vast bulk of radioactivity. In the UK, for instance, HLW amounted to less than 3 % of nuclear waste's volume, but almost 97 % of the inventory's radioactivity. Most of spent fuel has been moved into cooling pools (so-called wet storage) to reduce heat and radioactivity. As of 2016, 81 % of Europe's spent nuclear fuel is in wet storage, before being transferred to dry storage in separate facilities (see Section III.9.2.3).

A large share of the spent nuclear fuel stored in France and the Netherlands is planned to be reprocessed. Most other European nuclear countries have indefinitely suspended or terminated reprocessing [11].

The decommissioning of nuclear facilities will create additional very large amounts of nuclear waste. Excluding fuel chain facilities, Europe's power reactor fleet alone may generate at least another ∼1.4 million m^3 of nuclear waste from decommissioning.

To conclude, as of 2018, 142 nuclear power plants were in operation in Europe (excluding Russia

and Slovakia). The nuclear waste will continue to accumulate. Among them, HLW include elements with extremely long lifetimes (10^6 years). Because of their very high radiotoxicity level, these long-lived elements make challenging the processing of nuclear waste.

III.9.2.2 Spent fuel and radiotoxicity

To evaluate the environmental impact of nuclear waste, the notion of radiotoxicity is commonly used. It assesses the biological impact of ingesting or inhaling radionuclides.

The radiotoxicity R is expressed in sieverts[4] (Sv) and is written as

$$R = A(t)F_d \quad . \tag{III.9.4}$$

It quantifies the impact of the activity A of an element on body tissues, weighted by a dose factor F_d. This factor takes into account the type of radiation, the organ affected and the time the radionuclide spends in the body after inhalation or ingestion.
Figure III.9.4 shows the evolution over time of this quantity for different components of the spent fuel from a pressurised water reactor (PWR). It can be seen that the contribution of fission products (FP) is dominant during the first few centuries and then decreases sharply. This drop, around a thousand years, is due to the fact that the products of direct fission of uranium are mostly short-lived. However, FPs also include isotopes of iodine, caesium and technetium in smaller quantities, with half-lives greater than 100 000 years, which are considered as ILW. Heavy nuclei from the actinides[5] family (uranium-plutonium) dominate the long-term radiotoxicity of spent fuel. They are generally classified into two categories:

- The major actinides; uranium (U) and plutonium (Pu);
- The minor actinides (MA); in particular the isotopes of neptunium (Np), americium (Am) and curium (Cm).

This distinction between actinides is justified in particular by the much larger amount of major actinides at discharge and the the recycling potential of some of them (as in the case of Pu), whereas minor actinides are considered as waste. During core irradiation, neutron capture by heavy nuclei generates neutron-rich isotopes, which are likely to decay by β^- emission. These successive processes lead to the transuranics production, such as ^{239}Pu (the most abundant) from ^{238}U. Minor actinides are created by the capture and decay of uranium 238, as in the case of neptunium 237, which has a half-life of 2.14 million years. Its activity is nevertheless lower than that of americium isotopes. The ^{241}Am and ^{243}Am, which have half-lives of 430 years and 7400 years respectively, come from the plutonium formation chains. As

[4] The sievert is the unit of measurement of an equivalent dose. It takes into account the type of radiation affecting living tissue. It measures the amount of radiation absorbed by the material in gray (1 gray = 1 joule absorbed per kilogram of material). As an indication, the annual dose limits are 50 mSv/year for nuclear workers and 1 mSv/year for the public; natural irradiation is generally between 0.2 and 0.5 mSv/year.

[5] The actinide series comprises the chemical elements of the periodic table between actinium and lawrencium, with atomic numbers (Z) between 89 and 103 inclusive. In its natural state, uranium ($Z = 92$) and thorium ($Z = 90$) are relatively abundant. Elements with atomic numbers $Z > 92$ require neutron flux to be produced, such as the one present in reactor cores.

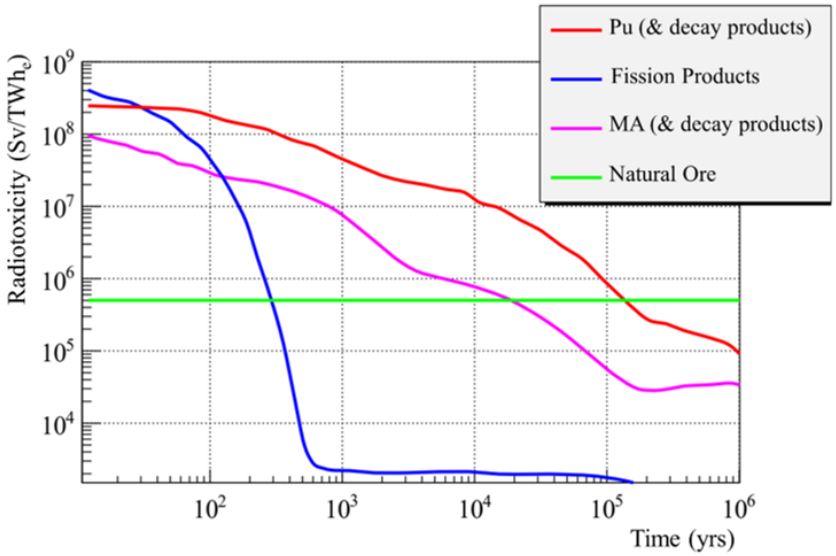

Fig. III.9.4: Evolution over time of radiotoxicity by ingestion of the different components of spent fuel from PWR [12, 13].

α emitters, minor actinides (MA) and plutonium are responsible for the long-term radiotoxicity of spent fuel.

III.9.2.3 Solutions, transmutation and incineration principle

Plutonium dominates the long-term radiotoxicity of spent fuel, long after most of the fission products have decayed. It also contains fissile isotopes with a high energy potential; fission of ^{239}Pu is considered more profitable in terms of neutrons than fission of ^{235}U. Strategies vary from one country to another. Two main management methods are currently considered.

The first is not to reprocess it and to store it permanently in surface, sub-surface or in deep geological disposal, after a prolonged period of storage in a pool for heat decrease. There are various reasons for this choice, including a security policy of non-proliferation and the absence of any industrial interest.

The second management strategy combines two approaches: part of the fuel is reprocessed to extract uranium and plutonium and the remaining part (fission products and minor actinides) is contained and stored. This is the case in France, for example, where U and Pu are considered as recoverable material. Part of it is reprocessed in the MOX (Mixed Oxide Fuel) used in $\sim$20 reactors.This recycling of Pu saves uranium ressources, but its implementation becomes more delicate after one cycle [14], due to the isotopic composition of Pu fuel and manufacturing issues. Using Pu fuel also increases the production of minor actinides.

In any case, the conditioning, transport, storage and disposal of nuclear waste constitute significant and growing challenges for all nuclear countries. Current national and international governances show a preference for geological disposal. Still, no country in the world has a deep geological repository in operation [11]. This solution also raises a societal issue, because of the associated risks of long-time disposal.

However, as Fig. III.9.5 illustrates, it would be possible to reduce the radiotoxicity (one to three

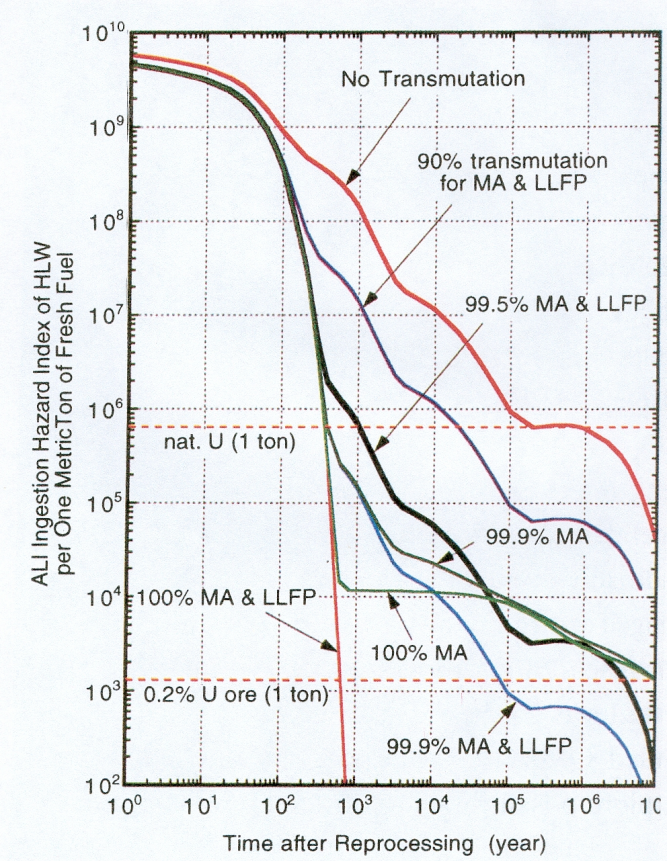

Fig. III.9.5: The effect of minor actinides (MA) and long-lived fission products (LLFP) removal on radiotoxicity (preliminary calculation) [15].

orders of magnitude) of the waste by transmuting at least 90% of them: in particular the MA which must be partitioned from the burnt fuel, and considering that U and Pu are reprocessed [15]. Transmutation would also minimize the surface of disposal site.

The transmutation principle, applied to nuclear waste, aims at modifying the nuclei of long-lived elements to transform long-lived radioactive isotopes into less radiotoxic elements, more stable or more readily fissile. Various types of particles (hadrons, photons) have been considered for artificial transmutation, but using neutron is the most efficient process. Nuclear reactors are therefore, a priori, suitable installations for transmutation, due to the presence of intense neutron flux.
The fission probability of an element varies according to the energy of the neutrons. Moreover, it is always in competition with other reactions, in particular the phenomenon of neutron capture. The latter is at the origin of the formation of MA, and successive captures of these nuclei generally lead to other MA. For transmutation, it is desirable to favour fission over capture in order to avoid the formation of higher-mass MA. As an example Fig. III.9.6 gives, the capture and fission cross-sections[6] for americium 241. For a neutron with energy of less than 1 eV (thermal neutron range), the capture cross-section

[6]The effective cross-section is a physical quantity related to the probability of interaction of a particle for a given reaction. The unit of effective cross-section is a unit of surface area the barn (b): $1\text{b} = 10^{-24}$ cm^2, i.e. the order of magnitude of an atomic nucleus size.

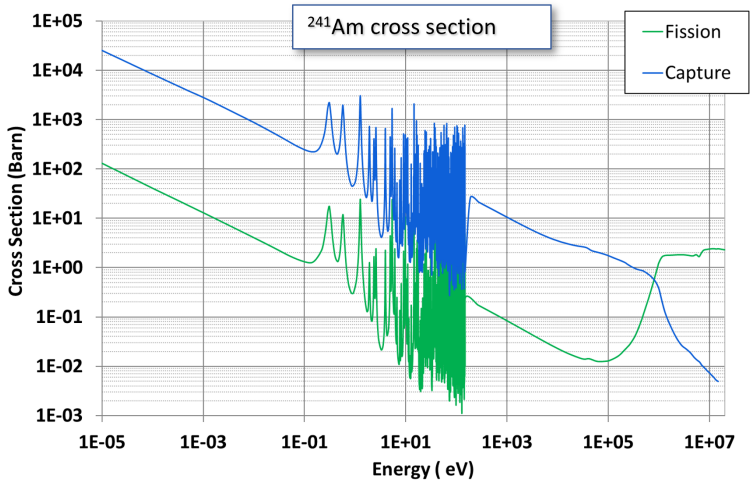

Fig. III.9.6: Capture (blue) and fission (green) cross sections of ^{241}Am as a function of neutron energy; from JEFF Nuclear Data library .

is predominant; capture is about a hundred times more likely than fission. This is also the case for energies between 1 eV and 1 MeV (the epithermal neutron range, where capture and fission occur at specific energy levels). Above 1 MeV (the fast neutron range), fission becomes more problable than capture.

The introduction of minor actinides or long-lived FP into the fuel has an influence on core reactivity, which can be linked to the effective multiplication factor, k_{eff}

$$k_{\text{eff}} = \frac{\text{Neutron production}}{\text{Neutron absorption and leakage}}. \tag{III.9.5}$$

The effective multiplication factor in a multiplying system represents the change in neutron population from one neutron generation to the next generation. k_{eff} is therefore the ratio of the neutrons produced by fission to the number of neutrons lost through absorption and leakage[7]. It drives the evolution of the neutron population for neutron flux at given energy spectrum:

- If $k_{\text{eff}} < 1$, in that case, the neutron population decreases in time and the chain reaction dies away. This condition is known as the subcritical state;
- If $k_{\text{eff}} = 1$, the population remains stable. This condition is the critical case, corresponding to a classical reactor in nominal operation;
- If $k_{\text{eff}} > 1$, the number of neutrons is exponentially increasing in time. This condition is known as the supercritical state.

From Fig. III.9.6, nuclear data show that to transmute nuclear waste such as minor actinides, the use of a thermal neutron spectrum is rather unfavourable. In fact, with a thermal spectrum, capture is favoured, and the waste to be burnt become too demanding in terms of neutrons. With a fast spectrum, the balance is more favourable and some nuclei, such as ^{237}Np and ^{241}Am, can be incinerated by fission [17].

[7] During the slowing down process and diffusion process some of the neutrons leak out of the boundaries of the reactor core; which affects the multiplication factor. It is mitigated with installation of reflectors inside, or at the edge of, the core.

Using a fast spectrum seems to be the best solution for heavy nuclear waste incineration. Still, the safety of a critical system then becomes more complicated to ensure. Indeed, it is difficult to introduce high proportions of minor actinides into the fuel of critical reactors; for kinetic reasons linked to the lower proportion of delayed neutrons and the low Doppler effect associated with these isotopes. In addition, although some incinerated products provide neutrons, they are mainly used for transmutation. To maintain criticality, an excess of neutrons must therefore be provided by conventional fuel, which also generates waste.

Consequently, using actual critical nuclear power reactors as incinerators means finding a compromise, which can be difficult, between incineration efficiency and safety: MA loading limit is $\lesssim 10\%$[8]. An alternative way of concentrating and burning waste efficiently in large quantities ($\sim 40\%$) [16] would be to use a reactor which is deliberately subcritical, but to which an external source of neutrons is added to maintain the power: i.e. an ADS (cf. FigIII.9.1).

III.9.3 ADS and high-power accelerators

As previously exposed in Section III.9.1, a hybrid reactor, driven by a proton accelerator and a spallation target, would allow the continuous injection of neutrons in order to maintain the nuclear power.

III.9.3.1 Spallation target

The spallation process can be described as follows. The interaction of a high-energy proton (at least several hundred MeV) with a thick target leads to significant neutron emission. As its energy is greater than the Coulomb barrier of the target nuclei, it causes nucleons to be ejected by intra-nuclear elastic scattering and the nuclei to become excited, de-exciting either by fission or by nucleon emission. The excited nuclei can also interact with other nuclei in the target, causing an inter-nuclear cascade reaction. These chains of reactions also produce nucleon emissions. Overall, these interactions are largely dominated by neutron emission. The heavier the target nuclei, the more efficient the spallation neutron production (cf. Fig. III.9.7). This production efficiency is also linked to the incident proton energy.

For ADS, a liquid spallation target is generally chosen to ease the cooling. The material commonly considered is a lead-bismuth eutectic (LBE), which has the advantage of a lower fusion temperature than lead alone (125°C compared with 325°C). The choice of the proton beam energy depends on several parameters, such as the required neutron energy spectrum, the deposited energy (heat) in the target, etc.

For an industrial-scale ADS the optimum neutron production is obtained for a proton beam energy within the 900 MeV–1.5 GeV range, as for example shown by the FEAT experiment [19]. At lower energy, protons tend to lose more energy by ionization, at the expense of the spallation process. Above $\sim$1 GeV, the spallation neutron production—and consequently the ADS energy gain—shows a plateau. It is also important to notice that the accelerator cost is related to its size, and therefore to the final beam energy. Compromises have to be made to optimise the ADS efficiency as regards its construction and operation costs. Once the beam energy chosen, the required beam power can also be adjusted with the beam current according to of the desired ADS power and nominal k_{eff}.

[8] Depending on how the MA are loaded into the reactor: in the core or in the blanket [13].

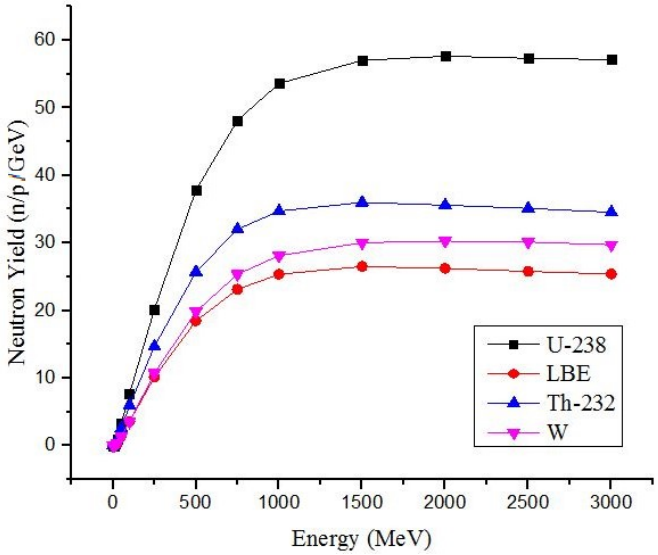

Fig. III.9.7: Comparison of the total number of spallation neutron yield per unit proton energy for U-238, Th-232, LBE and W-184 targets (simulations) [18].

III.9.3.2 Beam power requirements

In order to maintain the power in the subcritical core, the accelerator must provide a continuous wave (CW) of proton bunches. The first challenge for the accelerator is that it has to deliver a very high-power beam. The thermal power of the subcritical reactor, P_{th}, is function of the parameters of the spallation target, and the proton beam and k_{eff}. At first order, it can be written as [20]

$$P_{\mathrm{th}}(\mathrm{MW}) = E_{\mathrm{f}}(\mathrm{MeV}) \,.\, I(\mathrm{A}) \,.\, \frac{\xi_{\mathrm{spal}}}{\nu} \,.\, \frac{\varphi^* k_{\mathrm{eff}}}{1 - k_{\mathrm{eff}}}, \tag{III.9.6}$$

with

- E_{f}, the energy generated per fission ($\sim$200 MeV),
- I, the proton beam current,
- ξ_{spal} , the spallation target neutron yield per incident proton ($\sim$30, for a 1 GeV proton on a LBE target),
- ν the average number of neutrons emitted per fission ($\sim$2.5),
- k_{eff}, the effective neutron multiplication factor,
- φ^*, the source importance ($\sim$1.5) that characterises the efficiency of the external neutrons compared to fission neutrons, and thus the coupling quality (Source/Reactor).

This rather optimistic calculation - since it only gives a simplified behavior of the reactor's neutronic physics - enables to estimate the minimum required proton beam power.

Taking the example of an ADS demonstrator (i.e the MYRRHA project, cf. Section III.9.4.2.1), an effective multiplication factor of $k_{\mathrm{eff}} = 0.95$ is considered with a thermal power of the reactor of $P_{\mathrm{th}} = 100$ MW. A beam energy of 600 MeV will enable to provide a spallation neutron yield of $\xi_{\mathrm{spal}} \sim 15$ neutrons per incident proton. According to equation III.9.6, the minimum required beam

current for this demonstrator will be

$$I_{\mathrm{beam,mini,demo}} \approx 3\ \mathrm{mA}, \tag{III.9.7}$$

meaning a minimum required beam power of

$$P_{\mathrm{beam,mini,demo}} \approx 3 \times 0.6 = 1.8\ \mathrm{MW}. \tag{III.9.8}$$

For an industrial scale ADS a power of $P_{\mathrm{th}} = 1$ GW could be considered, with $k_{\mathrm{eff}} = 0.97$. Typically a proton beam energy of 1 GeV would be required to reach a spallation target yield of $\xi_{\mathrm{spal}} \sim 25$ neutrons per incident proton. Consequently the minimum required beam current for such industrial ADS would be

$$I_{\mathrm{beam,mini,indus}} \approx 10\ \mathrm{mA}, \tag{III.9.9}$$

meaning a minimum required beam power of

$$P_{\mathrm{beam,mini,indus}} \approx 10\ \mathrm{MW}. \tag{III.9.10}$$

The power depends on the transmutation strategy and objectives, and the number of ADS that will be installed. Still, in any case an ADS accelerator has to provide a CW "Megawatt-class" beam, making it one of the most powerful hadron accelerators in the world. The accelerator technology must also be quite versatile to adapt to the needs of the subcritical reactor.

III.9.3.3 High-power linacs and reliability

There is presently a growing demand for high-power hadron accelerators to better support various fields of science like particle physics, nuclear physics, or neutron-based physics. These applications require ever more efficient accelerators providing beams with very high mean power in the GeV energy range; while minimising power consumption and costs (construction and operation) [21]. This goes significantly beyond the present capability of most of existing facilities. In addition to the beam energy criterion, the need to produce an ever more intense flux of particles prevails. This results in an increase in the average intensity of the beams and therefore in their power. The panorama of high-power hadron accelerators is presently dominated by room-temperature machines as illustrated in Fig. III.9.8.

At present, there are two accelerators which are delivering a CW proton beam beyond ∼1 MW:

- The cyclotron of the Paul Scherrer Institute (PSI), which has the world's intensity record-breaking cyclotron, delivering 590 MeV protons of a few mA [23];
- The linac of the Spallation Neutron Source (SNS in Oak Ridge, USA), which recently delivered a beam power of ∼1.7 MW [24].

However, it should be noted that all future multi-Megawatt accelerators, whether planned (i.e. Chinese-ADS, SNS upgrade) or under construction (i.e. ESS, PIP-II), are now based on superconducting linac technology. Yet the cyclotron solution is a priori the most compact and cost-efficient layout

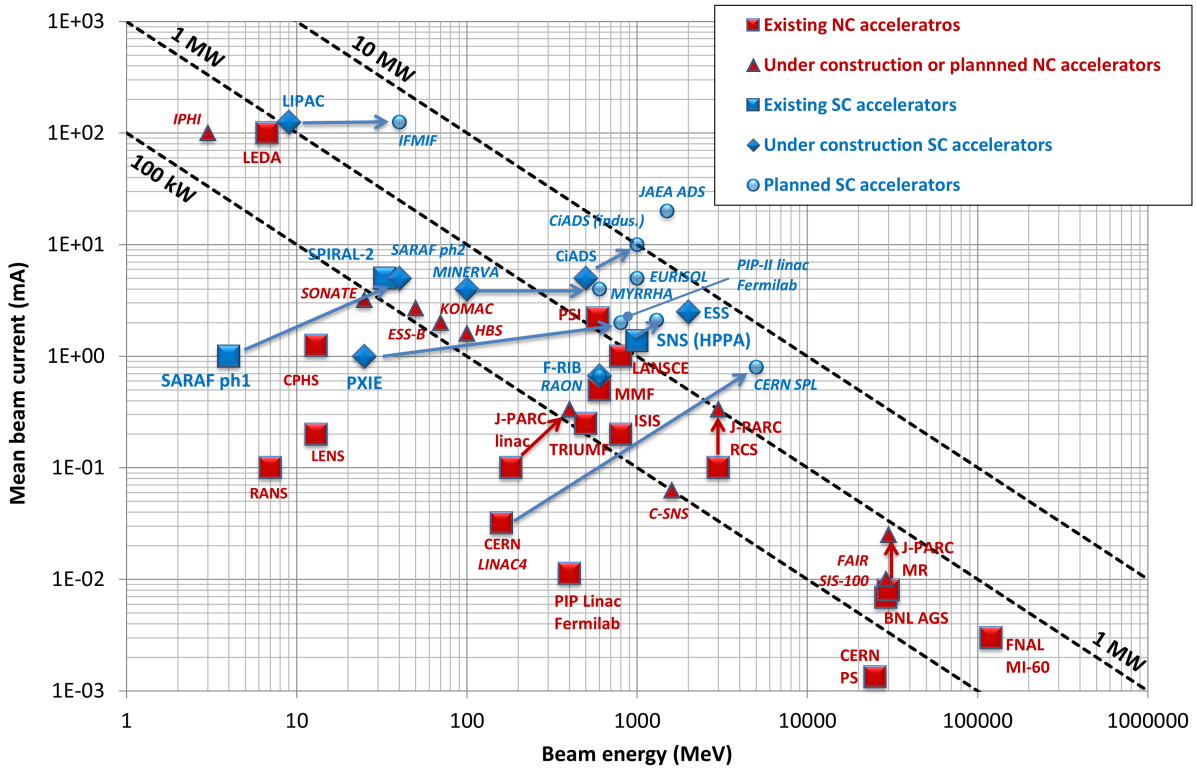

Fig. III.9.8: Panorama of high-power hadron beams worldwide (non exhaustive plot, updated from Ref. [22]).

and is further characterised by a good conversion efficiency of the RF (radio frequency) power to the CW beam. However, for an ADS demonstrator (and even more so for an industrial-scale one), providing a proton beam of tens of mA (and beyond) with a cyclotron remains debatable [25]. Furthermore, at energies close to 1 GeV, when protons become relativistic, we begin to reach the intrinsic limits of the cyclotron operating principle [27, 28]: as the particles speed increase, the relative gain in energy per revolution becomes smaller and smaller. Orbits separation is less significant, the extraction of a single-energy beam is more complex. Extraction of high-intensity beam in cyclotrons can lead to losses exceeding this threshold (typically 1 W/m for this high power machines). Furthermore, according to experience, electrostatic extraction and injection systems are subject to breakdown phenomena in the presence of a high-power proton beam, that strongly affect the machine availability, which is the main challenge for ADS. At this stage, a main drawback is also the absence of any strong vertical focusing, for example, through quadrupoles along the rather long (typically a few hundred meters) spiraling beam path : it provides a hard constraint on the possible intensity increase [25]. No construction attempt has ever been made in this range, but there exists studies [26] claiming that by pushing PSI technology to the extreme, one ultimately may reach $\sim$10 MW CW beam.

In contrast, linacs have a high intrinsic performance capability in terms of beam energy and current. Experience shows that they can deliver beams with peak currents of the order of a hundred mA (cf. Fig III.9.8). A linac consists of a chain of very similar (or identical) accelerating cavities. Each cavity provides an acceleration of a few MeV. The final energy, not limited by a basic physics principle,

is thus determined solely by the number of installed cavities. Of course, there are size and price considerations that act as practical limits. In addition, each cavity may be driven by its own RF system, with independent control of amplitude and phase for optimal settings. This offers great modularity and possibility to implement failure-compensation (cf. III.9.4.3) so as to maintain the accelerator operation. Thus, each cavity can provide a longitudinal beam focusing. Between the cavities, one can readily implement strong alternating-gradient (transverse) focusing, by means of quadrupoles.

To reach and exceed the MW range, superconducting RF (SRF) linear machines are becoming more and more mandatory, leading to several new superconducting accelerators being constructed or planned. One of the main reasons for using SRF accelerators is to minimize the overall power consumption and therefore to decrease the operating costs. But one has to keep in mind that this statement is not always true since it heavily depends on the operating RF or beam duty cycle (*dc*). In first approximation one can write the total power consumption, P_{total}, as

$$P_{\mathrm{total}} \approx dc \times (P_{\mathrm{beam}} + P_{\mathrm{cav}}) + P_{\mathrm{cryo}} \quad . \tag{III.9.11}$$

When dc approaches zero, P_{total} is dominated by the power required by the cryogenic plant P_{cryo}, which will in turn encourage to choose a full room-temperature solution. This straightforward statement suggests that for a given duty cycle, one can ideally find an optimal transition energy between the normal conducting (NC) and the superconducting (SC) structures of a given linac, which will minimize its overall power consumption. For high-power hadron linacs one can observe that the energy transition will be comprised between tens and hundreds of MeV. The higher the duty cycle is, the lower the transition energy will be [22].

But over and above the extreme beam power to be achieved, reliability is the key challenge to improve the performance of these "Megawatt-class" accelerators over the long term. Indeed, in order to optimise operating costs, the demands on beam availability are becoming increasingly stringent. A good example is the ESS project, where reliability objectives have been defined before the machine construction, based on user requirements. Figure III.9.9 shows the number of acceptable beam interruptions according to their duration (for an overall beam availability of 90%) [29]. The number of beam trips is compared with data from SNS over several years of operation. Data show that the ESS requirements for short interruptions (up to 6 minutes) appears to be achievable. However, the targets for longer outages (in excess of 20 minutes) are more restrictive than those achieved during SNS operation, even though the reliability of this linac is improving year after year [30].

These constraints are even more stringent for an ADS. The number of beam interruptions must be limited to very low values: one or two orders of magnitude compared with existing machines (cf. Fig. III.9.10). Indeed, beam interruptions lasting more than a few seconds could, if frequently repeated, induce thermal stresses on the highly irradiated materials of the window, target, fuel cladding or, more generally, reactor structures. Such beam interruptions, if systematically associated with a reactor shutdown, can also considerably reduce the availability of the installation: the ADS restart procedures could last $\sim$ 20 hours [31].

For MYRRHA, the present limit for the number of such beam interruptions has been set at 10 per 3-month operating cycle, with only interruptions lasting more than 3 seconds being counted. This

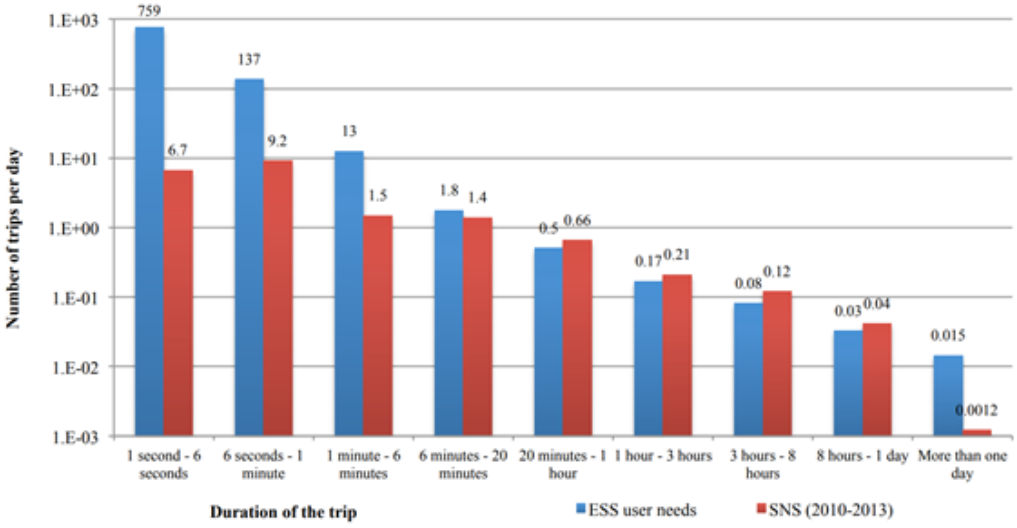

Fig. III.9.9: Maximum number of allowed beam trips for ESS (estimation) compared with SNS feedback (operation: 2010 to 2013) [29].

specification is largely based on the feedback from the PHENIX reactor [31]. However, other studies (for example the JAEA–ADS project [33], cf. Section III.9.4.2.3) report more flexible specifications, highlighting that there are still a number of uncertainties in this area, related in particular to the properties of irradiated materials, erosion and corrosion in the Pb-Bi environment, reactor restart procedures, etc.

In any case, the limit on the number of authorised beam interruptions will be significantly lower than the number of failures recorded on comparable accelerators in operation today, such as the SNS. This important difference (cf. Fig. III.9.10) shows that reliability is indeed the main challenge to ensure an efficient ADS operation. It also shows that the accelerator reliability and efficiency are improved during commissioning and operation (example of SNS linac). It should also be noted that SNS took ten years of operation to reach its design power [30], and performances continue to improve [24]. Consequently, to achieve the level of reliability required for the operation of an ADS, it is essential to address this issue from the design stage of the accelerator.

III.9.3.4 Accelerators features for ADS

To summarise, an ADS accelerator must meet specific and very stringent requirements to make the ADS technology suitable:

- It must provide a stable continuous CW beam power of few to tens MW, which is defined by the thermal power and subcriticality level of the reactor;
- The final beam energy range is about 500 MeV to 1.5 GeV for efficient neutron production through a spallation process, depending on subcritical reactor power (demonstrator or industrial);
- The beam current will range from few to tens of mA;
- The accelerator must operate with beam loss less than $\sim$1 W/m to ease maintenance, and avoid any beam stops triggered by the machine protection system;
- It has to operate with an extremely high reliability level to avoid thermal stress in the reactor

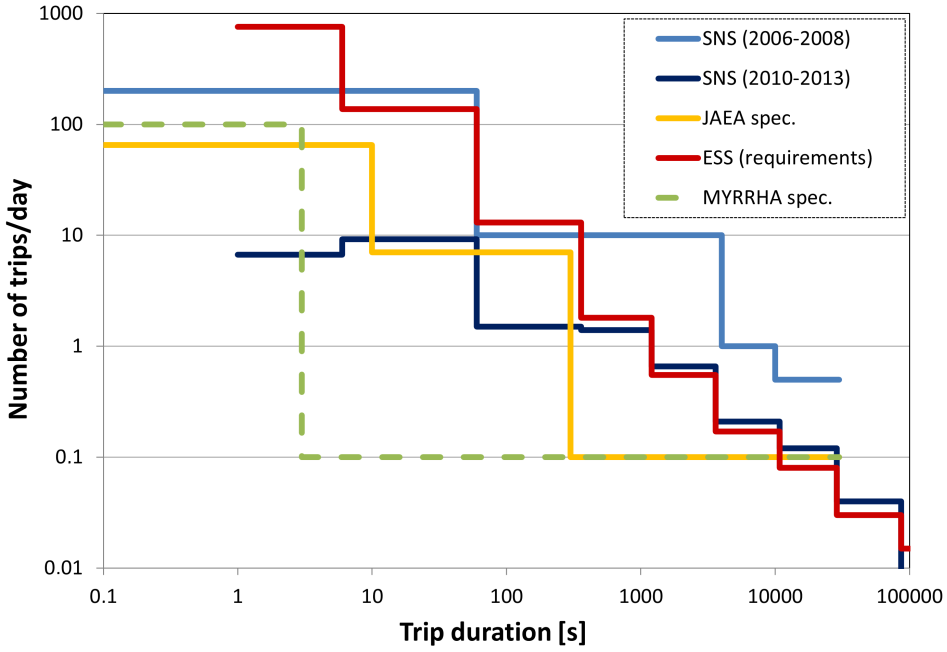

Fig. III.9.10: Beam trip frequencies as function of their duration for different machines (operation : SNS and specifications : ESS, JAEA ADS, MYRRHA) [29, 32, 33].

structures and ensure a high ADS availabiltiy. The number of allowed beam trips is more strict than for other high-power accelerators (Fig. III.9.10);

– A high beam stability is also necessary to guarantee the integrity of the beam window, that ensures the vacuum tightness between the accelerator pipes and the environment of the target/reactor core.

To this end most of the high-power ADS projects are based on the use of high-power superconducting linacs. These machines enable to implement redundant elements at all stages in order to provide a strong level of tolerance to faults, and therefore ensure a high level of reliability [34].

III.9.4 ADS projects and reliability-oriented R&D

ADS R&D is taking place around the world, and the particle accelerator community is pursuing high-reliability studies. These ADS projects are at different stage of development: from design to commissioning or operation stage. As summarised by B.Y. Rendon, the Table III.9.1 presents the overall situation on the ongoing worldwide activities at the beginning of year 2022 [35].

Table III.9.1: Summary of worldwide ADS activities [35].

	Accelerator	**Purpose**	**Status**
CiADS (China) [36]	2.5 (10) MW SRF proton linac	ADS demo	Commissioning
MYRRHA (Europe/Belgium) [37]	2.4 MW SRF proton linac	ADS demo	Construction
JAEA-ADS (Japan) [38]	30 MW SRF proton linac	Transmutation	Design
SKKU-ADS (Korea) [39]	5 MW SRF proton cyclotron	ADS Th based nuclear reactor	Design
KIPT (Ukraine) [40]	0.1 MW NC electron linac	ADS demo	Scientific prog. ongoing
IFSR (India) [41]	1 MW SRF proton linac	Energy prod.	Design
ADS-Troitsk (Russia) [42]	0.75 MW proton linac	ADS demo	Design (using existing Troitsk facility)
Mu*STAR (USA/Muons, Inc.) [43]	2.5 MW SRF proton linac	Transmutation	Design
CYCLADS (Europe/Consortium) [44]	5-10 MW proton cyclotron	Transmutation	Design

It is worth mentioning that even though the mainstream is the use of a proton linac, there are proposals to consider electron beams (KIPT) and cyclotrons (SKKU-ADS and CYCLADS). Nevertheless the main advanced programs for high-power demonstrators already in phase of construction/commissioning or advanced design are the CiADS, MYRRHA, and JAEA–ADS. They are all based on superconducting linac technology. A summary of the principal features and the current statutes of these three programs will be presented next (cf. Section III.9.4.2). Still one should also notice that several "close to zero power" facilities have been operated, in particular the GUINEVERE facility that has been in use for more than ten years.

III.9.4.1 GUINEVERE: a low-power ADS mock-up

The Generator of Uninterrupted Intense NEutrons at the lead VEnus Reactor (GUINEVERE) facility is devoted to experimental studies of ADS feasibility. It aims at investigating on-line reactivity monitoring, subcriticality determination, which are major safety issues, and operational procedures [45]. It is based on a subcritical reactor mock-up of SCK CEN (Mol, Belgium) modified into a fast lead subcritical core, VENUS-F. It is coupled to a versatile accelerator-driven neutron source developed by CNRS/IN2P3 (France). The accelerator operates in pulsed, continuous, or continuous with programmed interruptions beam mode, the latter being more representative of a powerful system.

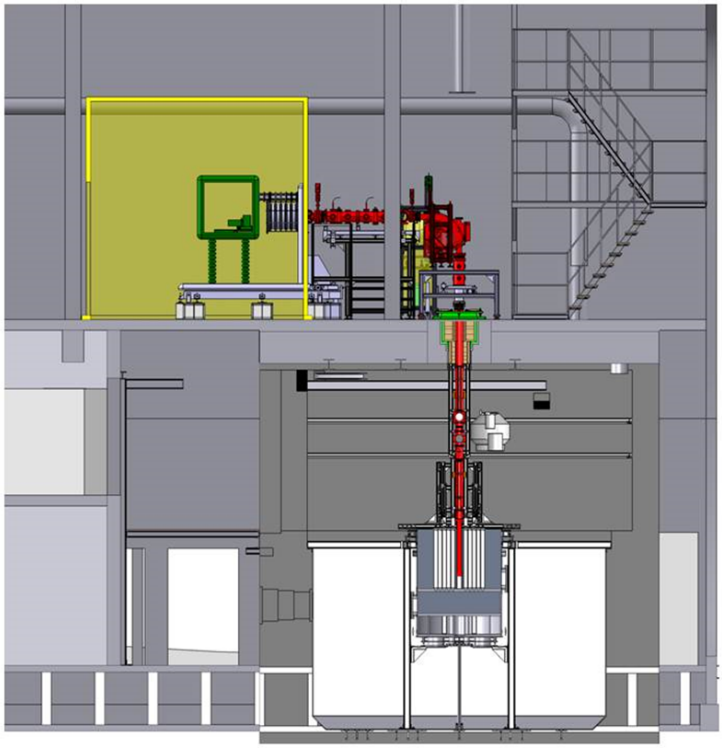

Fig. III.9.11: GUINEVERE facility layout (end section of the accelerator beam line inserted in the reactor core) [46].

Figure III.9.11 presents the layout of the facility. For subcritical operation, the VENUS-F reactor is loaded with 93 square fuel assemblies (FA). Each FA is composed of uranium metal highly enriched in ^{235}U (30 %) and solid lead rodlets acting as a fast system coolant. The cylindrical vessel is composed of a square casing containing layout of FA ($\sim$800 mm in diameter, $\sim$600 mm in height). It is surrounded by axial and radial lead reflectors. The central core region is left empty to host the terminal section of the accelerator beam line. This insertion channel holds a small lead buffer surrounding the beam pipe supporting the target. The reactor is also equipped with six safety rods and two control rods [45].

The "GEnérateur de NEutrons Pulsés Intense et Continu" (GENEPI-3C) is an electrostatic accelerator producing and transporting a deuteron beam onto a tritium target located at the core center, creating 14 MeV neutrons by T(d,n)^{4}He reactions. To fulfill the requirements of the experimental program, this machine produces alternatively (cf. TableIII.9.2):

– Short and intense deuteron pulses with adjustable repetition rate;
– Continuous (DC) beam, possibly chopped with adjustable programmable interruptions.

These beams with different time structures and intensities are generated by a duoplasmatron ion source. The main differences between pulsed and DC beam modes concern source efficiency and beam transport. The ion source and electrodes sit within a high-voltage platform and connect to the 250 kV accelerating structure. After a first horizontal beam-line section, a dipole magnet selects the D^+ ions and bends them down. Beam is transported vertically $\sim$7 m to the target at the core center (Fig. III.9.11). This 90° bend magnet, supported by a mobile frame, can be rolled away to lift up the vertical beam-

Table III.9.2: GENEPI-3C beam specifications [46].

Pulsed mode	**DC interrupted mode**
Beam bunches	With beam interruptions
I_{peak} ∼25 mA	I_{mean} : ∼50 µA to 1 mA
Rate: 10 Hz to 5kHz	Interruption rate: 0.1 to 200 Hz
Width ∼ 0.7 µs	Interruption duration: ∼20 µs to 10 ms
Reproducibility ∼1%	Interruption transition duration 1 µs

line section out of the reactor bunker for maintenance(cf. Fig. III.9.12). Beam transport is ensured using twelve electrostatic quadrupoles and four magnetic steerers.

Neutrons are produced in a thin layer of TiT (12 Ci) deposited on the target, where beam current and temperature are measured continuously. 14 MeV neutron rates are in excellent agreement with expectations, reaching 10^{11} n s^{-1} mA^{-1} (DC beam up to 1.1 mA). A cooling system dissipates the beam power (up to 250 W) using compressed air only.

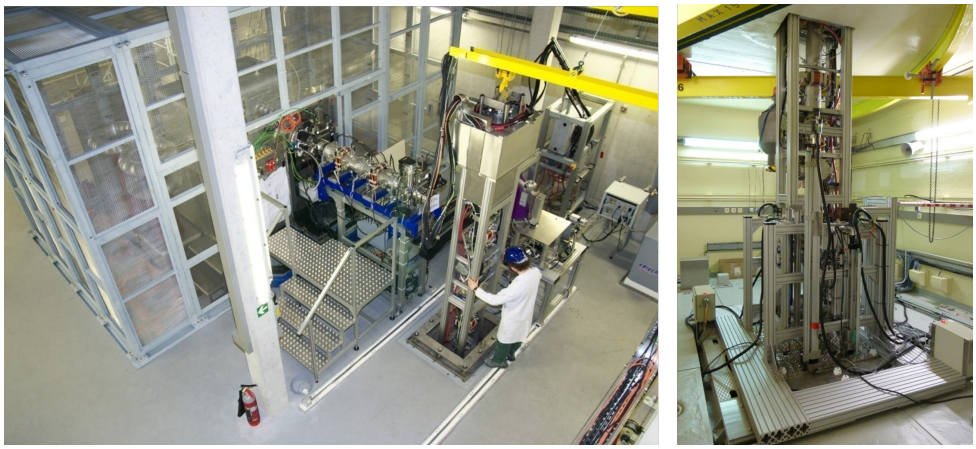

Fig. III.9.12: Left: upper level of the accelerator during beam line insertion. Right: vertical beam line inserted into the core [46].

GUINEVERE provides a unique facility in Europe for fast subcritical reactor physics investigations. The project was initiated in 2006, and the facility has been fully commissioned and under operation for experimental reactor physics since 2011. It has been used to study, develop and establish methods to monitor the reactivity of a subcritical core [12, 47–50], in order to ensure the operation of high-power ADS.

III.9.4.2 Main ADS projects

III.9.4.2.1 MYRRHA

The MYRRHA project, led by SCK CEN, aims to build an ADS demonstrator with a capacity of 50–100 MW_{th}. The main objectives of the design of this installation will be:

– To demonstrate the control of an ADS at significant power, as well as study transmutation feasi-

bility of long-lived radionuclides;

– To serve as a high-flux, fast-spectrum irradiation platform, enabling the study of materials for fast fission neutron reactors and fusion reactors, or for the production of radioisotopes for medical applications;
– To contribute to the demonstration of liquid molten-lead Generation IV fast-reactor technology.

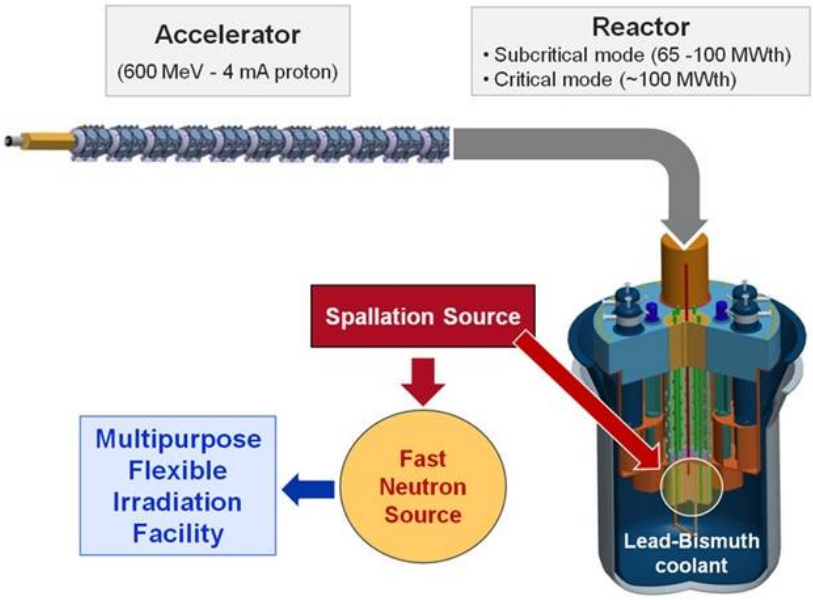

Fig. III.9.13: MYRRHA priciple scheme.

The conceptual principle of the machine is described in Fig. III.9.13. This fast neutron reactor will be able to operate in both critical and subcritical modes. The fuel will be MOX into which irradiation and transmutation test cells will be inserted. In subcritical mode, the external neutron source is supplied by a proton beam impiging a spallation target through an isolation window. The spallation target is a lead-bismuth eutectic (Pb-Bi). Liquid Pb-Bi will also be used as heat transfer fluid for the reactor cooling loop.

The MYRRHA construction is now following a phasing approach. The first phase (called MINERVA) consists in building and operating the linac limited to a 100 MeV final beam energy. The aim will be to experimentally investigate the feasibility and efficiency of the linac reliability and fault tolerance schemes (see Section III.9.4.3). The beam will also be transported to independent target stations, one for radio-isotope research and production of radio-isotopes for medical purposes, the other one for fusion materials research [51, 52].

MYRRHA will accelerate a 4 mA CW proton beam to a final energy of 600 MeV (cf. Fig. III.9.14). Table III.9.3 summarizes the most relevant parameters of the project. This linac will comprise three main parts:

– An injector (redundant for reliability purpose, seeSection III.9.4.3) that accelerates the beam to 17 MeV. The construction of the injector already started and has been commissioned [53, 54];

– A medium energy transport line (MEBT) to bring the beam to the superconducting linac;
– A superconducting linac to accelerate the beam up to 600 MeV.

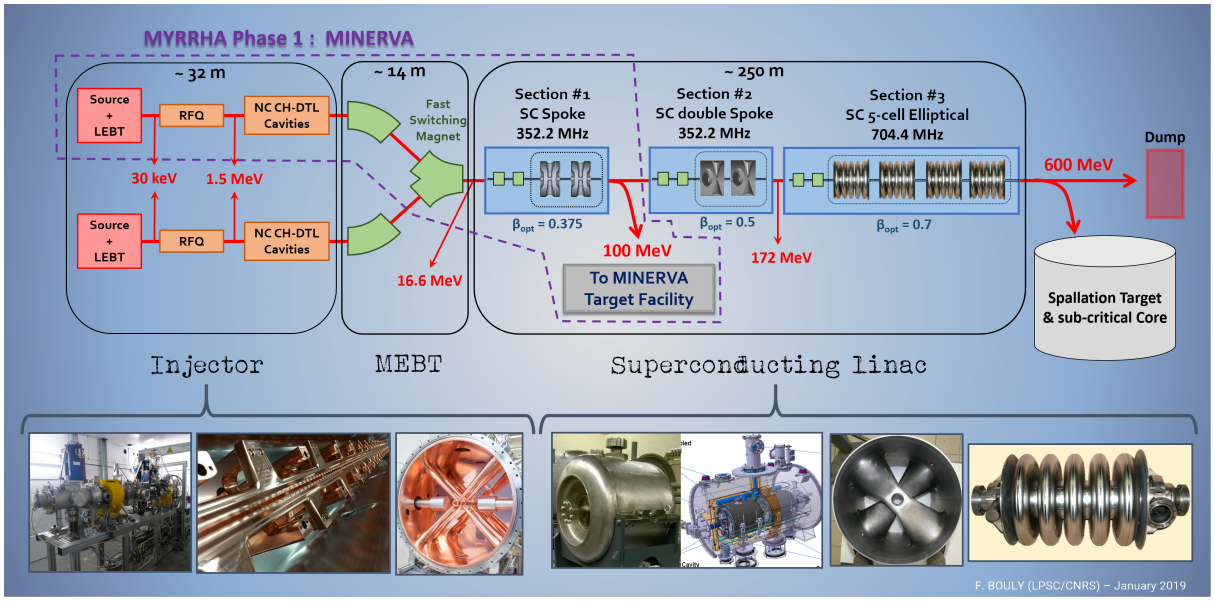

Fig. III.9.14: MYRRHA and MINERVA linac scheme [55].

The superconducting cavities of the main linac are independently powered with high-energy acceptance and moderate energy gain per cavity (low number of cells and very conservative accelerating gradients), the goal being to increase as much as possible the tuning flexibility and to provide sufficient margins for the implementation of the fault-tolerance scheme. This aspect will be discussed in Section III.9.4.3.

III.9.4.2.2 CiADS

China Initiative Accelerator Driven System (CiADS) is phase II of the Chinese ADS program [36, 56]. CiADS will employ a superconducting CW linac to accelerate 5 mA proton beam to a final energy of 500 MeV (cf. Table III.9.3), as shown in Fig. III.9.15. CiADS is led by the Institute of Modern Physics (IMP) in collaboration with the Institute of High Energy Physics (IHEP), China National Nuclear Corporation (CNCC), and China General Nuclear Power Group (CGN) and will be located in Huizhou, China.

Fig. III.9.15: CiADS linac [56].

IMP is currently commissioning the ADS Front-end Demo Facility (CAFe), which was constructed together with IHEP. The CAFe aims to demonstrate the superconducting front-end linac 10 mA CW beam for CiADS (cf. Fig. III.9.16). A high beam power test was conducted from January to March 2021, achieving a beam power of 205.5 kW with a 10.2 mA CW proton beam, which makes probably CiADS the most advanced program in the construction of an ADS-like accelerator. CiADS works on various activities: RFQ manufacturing and improvements, Superconducting RF, solid-state amplifiers, superconducting solenoids, and LBE target, as well as reliability-oriented design studies.

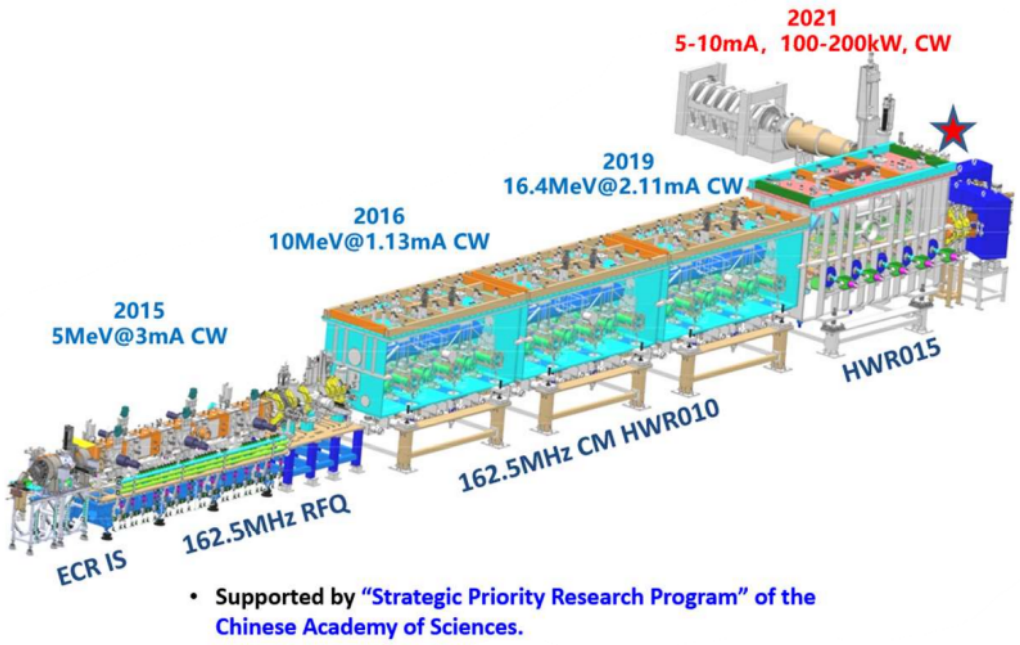

Fig. III.9.16: CiADS Front-end demo facility [56].

III.9.4.2.3 JAEA–ADS

The Japan Atomic Energy Agency (JAEA) is working on the design of a 30 MW CW proton linac for the ADS project [38]. The JAEA–ADS linac will accelerate a 20 mA proton beam to a final energy of 1.5 GeV (cf. Fig. III.9.17). Then, the beam will be transported to the spallation target placed inside the 800 MW_{th} thermal power subcritical reactor (cf. parameters in Table III.9.3). JAEA has a plan to construct a transmutation experimental facility (TEF) and is working on the LBE target system, shielding calculations as well as reactor design [35].

The linac team is focusing on two topics: beam optics and SRF prototyping. For SRF fabrication, the prototyping of the single spoke resonator—that will constitute section SSR1 (18 to 50 MeV)—is taking place [58]. Finally beam-optics studies have been focused on reference design and dedicated studies have been carried out on fast beam-recovery scenarios [59–61].

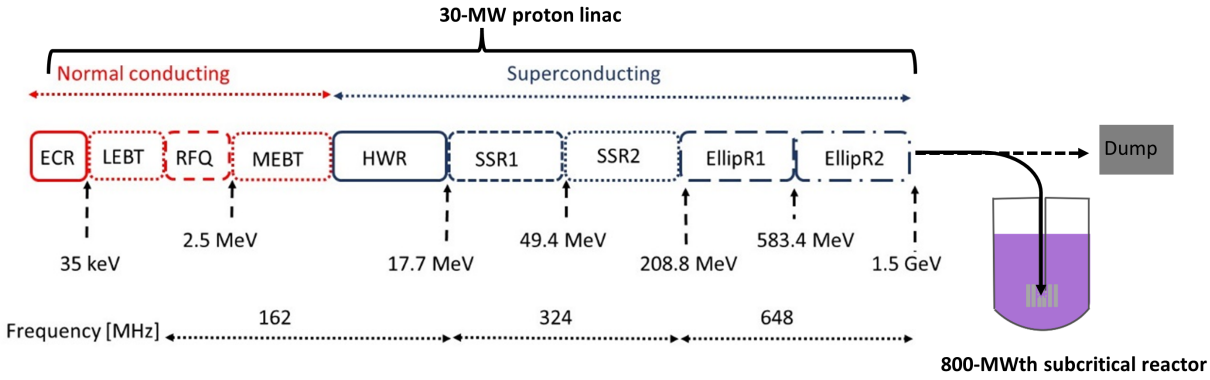

Fig. III.9.17: JAEA–ADS layout [59].

Table III.9.3: Design parameters summary for the main on-going ADS projects [35].

	Parameter	CiADS	MYRRHA	JAEA-ADS
Proton linac	Energy (GeV)	0.5	0.6	1.5
	Beam current (mA)	5	4	20
	Operation mode	CW/pulse	CW	CW
	RF Frequency (MHz)	162.5/325/650	176.1/352.2/704.4	162/324/648
Target	Maximum beam power (MW)	2.5	2.4	30
	Material		lead-bismuth eutectic (LBE)	
Fast reactor	k_{eff}	∼0.75/∼0.96	0.95	0.97
	Thermal power (MW)	∼7.5/∼9.7	50-100	800

III.9.4.3 Reliability-oriented R&D and fault compensation

III.9.4.3.1 Fault-tolerance concept

As previously assessed, the challenge for these high-power linacs is their expected extremely high level of reliability. To minimise or avoid beam trips longer than a few seconds during operation it is necessary to design ADS linacs with reliability guidelines. These guidelines can be summarised as follow:

- Provide a strong and robust beam-optics design , with elements (especially accelerating cavities) operating derated as regard to their maxium capabilities (margins on the accelerating field, E_{acc});
- Provide an efficient maintenance scheme, with possibility to repair failed systems while the operation of the machine is going on;
- And finally introduce redundancy wherever possible to be able to tolerate or mitigate failures.

Redundancy is a key concept for implementing 'fault tolerance' in the ADS accelerator.

Parallel redundancy uses two elements to ensure a single function. This is for example the adopted philosophy for the MYRRHA injector (Fig. III.9.14). Since each element is unique in the injector (RFQ, DTL cavities, etc.), if one them fails it cannot be compensated by the neighboring ones. Therefore the strategy is to dispose of a second "hot" stand-by spare injector. If a fault is localised in the first injector, the polarity of the MEBT switching magnet is reversed in a few seconds. The beam is then

resumed using the second injector. It is of course supposed that beam tuning of Injector 2 has been previously performed. The failed Injector 1 should then be repaired as soon as possible, during operation if possible. Still for economic reasons, this mitigation scenario should clearly be kept to a minimum.

Serial redundancy, on the other hand, replaces the functionality of a missing element by readjusting adjacent elements with identical functionality. It is closely linked to a modular structure. The architecture of a superconducting linac consists of a sequence of nearly identical modular RF cavities and cryomodules. The key for implementing the fault tolerance concept is here clearly serial redundancy, where a missing element's functionality can be replaced by retuning other elements with nearly identical functionalities. Such a fault-tolerance scheme can typically be applied to RF cavities which are known to be elements rather sensitive to failure[9] during long operation periods. Several reliability and beam dynamics studies have already been performed [64,65] to assess the feasibility of failure compensation. Still, several conditions must be implemented in the linac design to be able to apply such failure-compensation scheme:

- Each accelerating cavity needs to be independently controlled in amplitude and phase;
- Beam dynamics need to be tolerant enough to allow the presence of inactive cavities (or focusing elements) and accommodate the subsequent retuning of corrective cavities (or focusing elements) without loss of the nominal beam properties. Therefore the linac acceptance needs to be as large as possible;
- The nominal design and tuning of the linac should have been foreseen with margins on the RF accelerating voltage and phase (typically 30% on E_{acc}).

III.9.4.3.2 Cavity failure compensation

One should be reminded that these high-power linacs handle non-relativistic proton beams. Consequently any RF-cavity fault implying beam energy loss will also lead to a phase slip along the linac. As it will increase with distance, it will thus push the beam out of the stability region: the beam will be completely lost.
To recover such RF-fault conditions, the philosophy is to re-adjust the accelerating fields and phases of some non-faulty RF cavities to recover the nominal beam characteristics at the end of the linac, and in particular its transmission, phase and energy.

From this statement there are several possible ways to compensate a cavity failure. A first one would be to retune the phase of all the cavities which are placed downstream the failed one and potentially increase the gradient of some of them to recover the energy.
This **global compensation** strategy presents the advantage to redistribute constraints over a large number of cavities. In this way there is no specific need to have high operation margins on the accelerating field of the cavities. The disadvantage is the large number of cavities (tens to one hundred) that have to be re-tuned in a very short time (a few seconds for an ADS). The risk of setting error (due to calibration, measurement uncertainties, etc.) is also multiplied. Nevertheless this procedure has been recently demonstrated at SNS : one cavity was switched off and the whole linac was re-tuned in a few minutes [62].

[9] As well as their associated systems : RF amplifiers, cooling and cryogenic systems, etc.

The other approach is to apply a **local compensation** scheme as illustrated by Fig. III.9.18. This local compensation method presents the advantage of involving only a small number of elements. Therefore it is possible to compensate for multiple RF faults in different sections of the machine at the same time. But it brings more constraints on the compensation cavities since they will have to be quickly retuned with high gradient changes. Several studies assessed the feasibility of such fast retuning procedures [63, 65]. But, it also means that the RF system and RF amplifer have to be over-designed (large RF margins) in order to apply the retuning procedures, which will increase the cost of the machine.

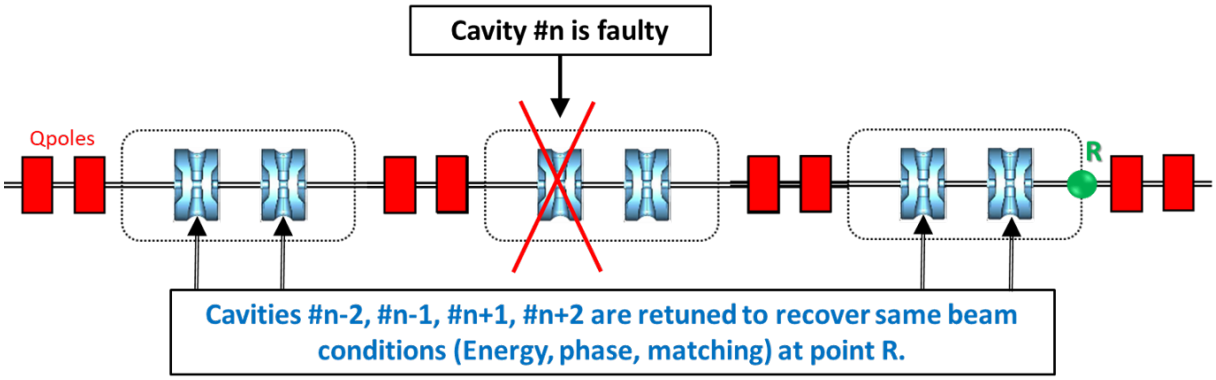

Fig. III.9.18: Principle of a local compensation methods.

In practice this scenario uses the following sequence, to be performed in less than a few seconds:

1. A fault is detected somewhere in the linac, and the beam is immediately and automatically stopped at the source exit by the machine protection system;
2. The fault is localized in the RF loop of a superconducting cavity by the fault diagnostic system;
3. The field and phase set-points are updated in some RF cavities adjacent to the failed one. These set-points need to be determined previously during the commissioning phase, and possibly stored directly in digital chips in the Low Level RF (LLRF) systems;
4. To avoid any beam-loading effect, the failed cavity is detuned by a few hundred bandwidths using a suitable mechanical tuning system, possibly with piezoelectric actuators. This sequence is the most demanding in terms of time duration;
5. Once steady state is reached, the beam is resumed. The failed RF system should then be repaired as soon as possible, during operation if possible, and put back on line using a similar reverse procedure.

As an application example, Fig. III.9.19 shows the results of beam dynamics studies for multiple failure compensation in the superconducting linac of MYRRHA. Local compensation is applied to compensate 10 failed cavities distributed along the linac. In the last part of the linac a full cryomodule failure is considered : meaning 4 adjacent cavities are not usable anymore. In that case the failure is compensated with two cryomodules placed upstream and two cryomodules placed downstream the failed one, i.e. 16 compensation cavities. The new accelerating voltage and phase settings are calculated with a beam dynamics tool especially developed for failure compensation methods [64]. The beam energy is recovered and no loss is observed in the simulations. This is illustrated by Fig. III.9.20 showing the

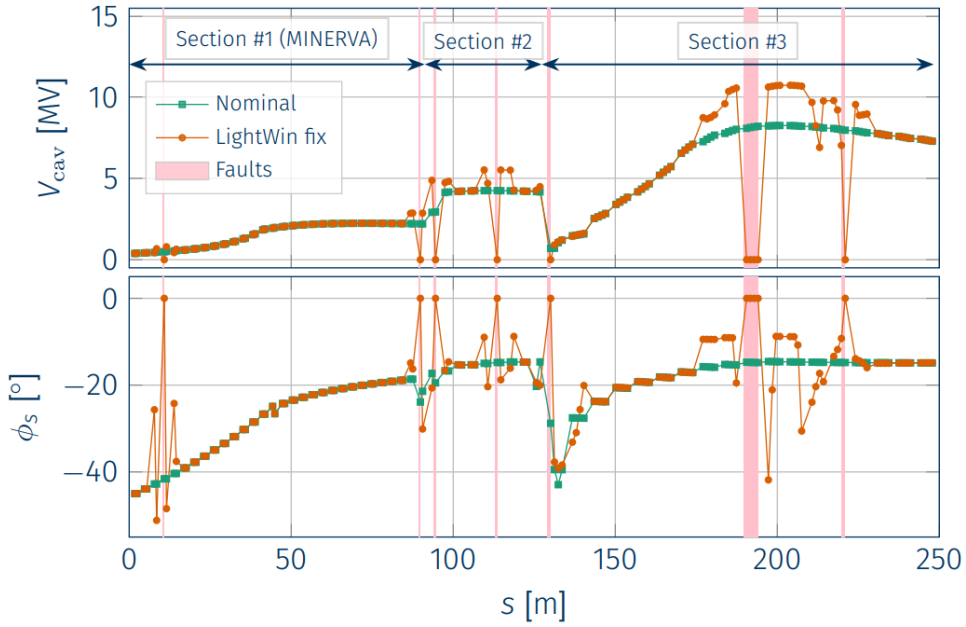

Fig. III.9.19: Simulation of accelerating voltage and synchronous phase of MYRRHA linac, in nominal and compensated cases. For the compensation case, there are 10 cavities off out of a total of 150 [64].

particle distributions along the linac. The "bumps" on the energy and phase distribution of the particles show the discrepancies of the beam centroid in the longitudinal plane as regard to the nominal tuning (no failure). After each retuning zone the energy and the phase of the beam are recovered, meaning that the bunches remain synchronised with the RF field of the cavities that did not have to be retuned.

These advanced beam dynamics studies show that such retuning scenarios can be applied on high-power superconducting linacs. Presently a strong effort is made to develop tools enabling automatic calculation of any failure scenario. The aim is to anticipate—as much as possible—any failure scenario, by creating a failure compensation database. Thus, once a cavity failure is detected by the global control system of the machine, the fault-compensation settings can be quickly applied to the compensation cavities. In addition, the tool should precisely reproduce the beam physics, with efficient algorithms to re-calculate the database if some tunings are modified during the machine operation.

Theses advanced beam-dynamics studies also enable to assess the limits of retuning methods [65]. For example, Fig. III.9.21 shows the effect of multiple failure compensations on the longitudinal acceptance on the JAEA–ADS linac. This acceptance decreases and one should be careful to limit emittance growth. There is a risk of particles "escaping" from the stable zone in the longitudinal plane. In that case they de-synchronise with RF and create unexpected losses. All this confirms that to ensure an "ADS-like" linac operation with a high reliability level, it is necessary to address this issue from the very beginning of the accelerator design.

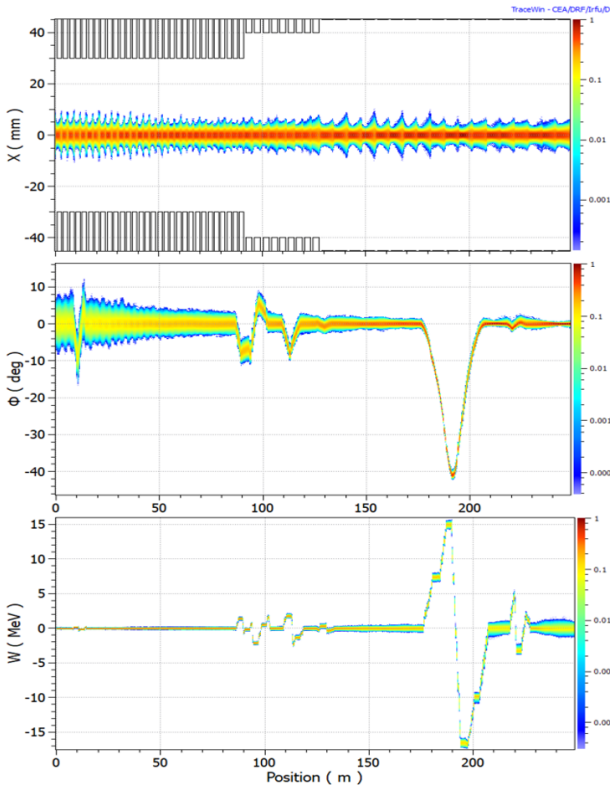

Fig. III.9.20: Beam dynamics and beam distributions with failure compensation along the MYRRHA linac, tracking with 10^6 macro-particles.

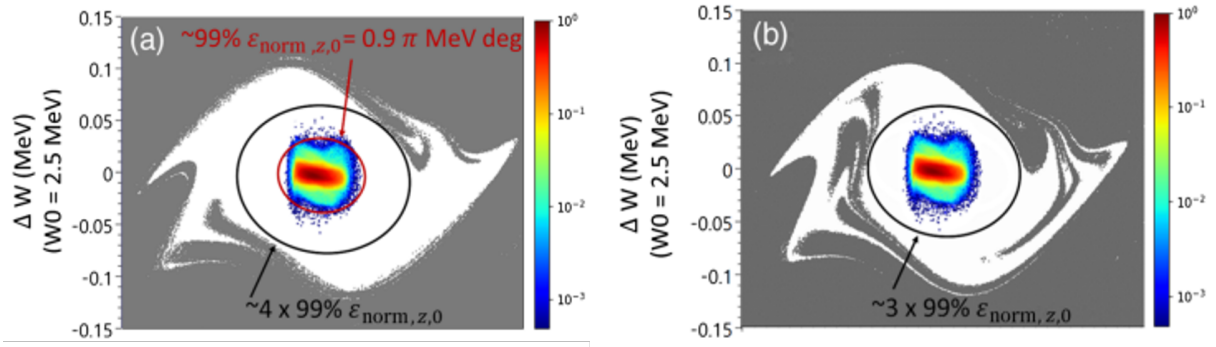

Fig. III.9.21: Longitudinal acceptance of the JAEA main linac for the different cases: (a) baseline (nominal tunings), (b) multiple SRF cavity failures in independent periods [60].

III.9.5 Conclusions

Nuclear-waste management is a long term and complex issue. It also significantly depends on the policies of individual countries with regard to energy production. Still, the amount of long-lived nuclear waste is growing worldwide. One of the favored solution would be long-term deep geological repository for spent nuclear fuel. But to date no country has a final HLW disposal site in operation yet. The high level of radio-toxicity of long-lived waste, and the large amount of heat they release, have an impact on the reliability of the repositories.

In this context, a possible strategy is to reduce the volume and life time of the most radiotoxic isotopes in order to ease their long-term management. To do so Accelerator Driven Systems appear as a potential solution to fission significant amount of minor actinides.
To operate efficiently an ADS requires a proton beam in the 500 MeV–1.5 GeV energy range with a beam power varying from a few to tens of MW. The most advanced solution to provide such a beam is to use a superconducting linac. The reliability of this superconducting linac is crucial to ensure an efficient ADS operation. This condition certainly represents the major technological challenge for such high-power linac, as no other proton accelerator in the world has reached it yet. At the present, ADS accelerators have benefited from the current state-of-the-art of the high-power accelerator in operation. However, a major effort is made in the community to improve the availability and the reliability of high-power accelerators. ADS R&D enabled to develop new approaches for designing (redundancy) and tuning (fault-compensation) high power linacs that could be beneficial for the whole accelerator community.

Finally, implementing a transmutation strategy in a country such as France would require $\sim$ 10 to 20 ADS [66]. It is clear that the associated cost of such development can represent an obstacle. In addition, this solution also implies the implementation of a dedicated partitioning industry, the manufacturing of MA-enriched fuel, and it also requires to maintain these fuels for at least 100 years in reactors. All these issues contribute to postpone the decision on implementation of the transmutation option.

Acknowledgement

Author would like to sincerely thank Dr. Annick Billebaud (LPSC/CNRS) for her advise and her precious feedback, as well as Dr. Bruce Yee-Rendon (J-PARC/JAEA) and Dr. Maud Baylac (LPSC/CNRS) for their help.

References

[1] C.M. Van Atta, Brief history of the MTA project (UCRL–79151). United States, Jan 1977, https://inis.iaea.org/search/search.aspx?orig_q=RN:8322162.

[2] W.B. Lewis, The significance of the yield of neutrons from heavy nuclei excited to high energies, Atomic Energy of Canada Ltd., AECL-968 (1952).

[3] J.-P. Revol, Accelerator-Driven Systems (ADS) Physics and Motivations, In: Thorium energy for the world, Springer, Cham, 2016, Eds. J.-P. Revol *et al.*, pp. 235–242, doi:10.1007/978-3-319-26542-1-35.

[4] G.J. Van Tuyle *et al.*, The PHOENIX Concept, Brookhaven National Lab. (BNL), Upton, doi:10.2172/6021439.

[5] N. Nakamura *et al.*, Present status of the OMEGA program in Japan, in Proc. Second OECD/NEA Information Exchange Meeting on Actinide and Fission Product Separation and Transmutation, Argonne, 11–13 Nov 1992, Proc.92-OECD/NEA-IEMAFPST.

[6] C. Rubbia, A high gain energy amplifier operated with fast neutrons, *AIP Conf. Proc.* **346** (1995) 44–53 (1995), doi:10.1063/1.49069.

[7] Conversion factors and energy equivalents, 2004 survey of energy resources, 20th ed., Eds. J. Trinnaman and A. Clarke, Elsevier Science, Oxford, 2004, doi:10.1016/B978-008044410-9/50023-1.

[8] International Energy Agency, Energy Statistics Data Browser, IEA, Paris, 2023, https://www.iea.org/data-and-statistics/data-tools/energy-statistics-data-browser, last accessed 21 Oct. 2024.

[9] ANDRA, Les essentiels - Inventaire nationaldes matières et déchets radioactifs, 2020, ANDRA Report 2020.

[10] International Atomic Energy Agency (IAEA), Classification of Radioactive Waste: General Safety Guide GSG-1, 2009, ISBN 978–92–0–109209–0.

[11] The World Nuclear Waste Report, Focus Europe, 2019 Berlin and Brussels, WNWR-2019.

[12] T. Chevret, Mesure de la réactivité de réacteurs sous-critiques pilotés par accélérateur par l'analyse d'expériences d'interruptions de faisceau programmées, Université de Caen Normandie, Phd Thesis, 2016, tel-01431421.

[13] CEA, Tome 2, Séparation-Transmutation des éléments radioactifs à vie longue - Rapport sur la gestion durable des matières nucléaires, 2012, CEA-T2-2012.

[14] S. Sala and M. Salvatores, Réduction de la Radiotoxicité des Déchets Nucléaires à vie longue: Etudes Théoriques et Stratégiques de la Transmutation des Actinides Mineurs et des Produits de Fission dans les réacteurs électronucléaires, 1995.

[15] M. Furusaka *et al.*, The Joint Project for High-Intensity Proton Accelerators, Nippon Genshiryoku Kenkyujo JAERI, 1999 AERI-Tech-99-056 .

[16] Z.Chen, Y. Wu, B. Yuan and D. Pan, Nuclear waste transmutation performance assessment of an accelerator driven subcritical reactor for waste transmutation (ADS-NWT), Annals of Nuclear Energy, Volume 75, 2015, Pages 723-727, ISSN 0306-4549, doi:10.1016/j.anucene.2014.09.002.

[17] A. Zaetta, Transmutation is technically feasible, Spring 2002, Clefs CEA,(46):34-39.

[18] M. A. Amirkhani, M. Hassanzadeh and S. A. Safari, A simulation study on neutronic behavior of non-fissionable and fissionable materials of different geometries as spallation targets in ADS, *Rad. Phys. Eng.* **1** (2020) 29–36, doi: 10.22034/rpe.2020.89329.

[19] S. Andriamonje *et al.*, Experimental determination of the energy generated in nuclear cascades by a high energy beam, *Phys. Lett. B*, **348** (1995) 697–709, doi:10.1016/0370-2693(95)00154-D.

[20] A. Billebaud, Réacteurs hybrides : Avancées récentes pour un démonstrateur, École thématique, Ecole Internationale Joliot-Curie de Physique Nucléaire, Maubuisson, 18–23 Sep. 2006, 2007, ⟨cel-00139971⟩.

[21] M. Seidel, "Towards Efficient Particle Accelerators - A Review", in *Proc. IPAC'22*, Bangkok, Thailand, Jun. 2022, pp.3141–3146, doi:10.18429/JACoW-IPAC2022-FRPLYGD1.

[22] J.-L. Biarrotte, "High Power Proton/Deuteron Accelerators", in *Proc. SRF'13*, Paris, France, Sep. 2013, pp. 35–41. paper MOIOB01.

[23] M. Seidel *et al.*, "Production of a 1.3 MW Proton Beam at PSI", in *Proc. IPAC'10*, Kyoto, Japan, May 2010, pp. 1309–1313, paper TUYRA03.

[24] F.C. Pilat, "SNS Upgrade and Power Ramp Up", in *Proc. HB2023*, CERN, Switzerland, oct. 2023, THC1I1.

[25] A.C.Mueller, Review of Accelerators for Accelerator-Driven Systems (ADS), In: Thorium energy for the world, Springer, Cham, 2016, Eds. J.-P. Revol *et al.*, pp. 243–248, doi:10.1007/978-3-319-26542-1-36.

[26] Th. Stammbach, *et al.*, The feasibility of high power cyclotrons, Nuclear Instruments and Methods in Physics Research Section B: Beam Interactions with Materials and Atoms, Volume 113, Issues 1–4, 1996, Pages 1-7, ISSN 0168-583X, doi:10.1016/0168-583X(95)01377-6.

[27] A. Kolano, *et al.*, Intensity limits of the PSI Injector II cyclotron, Nuclear Instruments and Methods in Physics Research Section A: Accelerators, Spectrometers, Detectors and Associated Equipment, Volume 885, 2018, Pages 54-59, ISSN 0168-9002, doi:10.1016/j.nima.2017.12.045.

[28] D. Winklehner, A. Adelmann, J. R. Alonso, L. Calabretta, H. Okuno, T. Planche andvM. Haj Tahar, Report of the Snowmass'21 Workshop on High-Power Cyclotrons and FFAs, 2022, doi:10.48550/arXiv.2203.07919.

[29] E. Bargallo *et al.*, "ESS Availability and Reliability Approach", in *Proc. IPAC'15*, Richmond, VA, USA, May 2015, pp. 1033–1035, doi:10.18429/JACoW-IPAC2015-MOPTY045.

[30] J. Galambos, "Operations Experience of SNS at 1.4MW and Upgrade Plans for Doubling the Beam Power", in *Proc. IPAC'19*, Melbourne, Australia, May 2019, pp. 4380–4384 doi:10.18429/JACoW-IPAC2019-FRXPLM1.

[31] G. Rimpault *et al.*, The Issue of Accelerator Beam Trips for Efficient ADS Operation, Nuclear Technology, 2017, 184 (2), pp. 249–260, doi:10.13182/NT12-75.

[32] D. Vandeplassche and L. Medeiros-Romao, "Accelerator Driven Systems", in *Proc. IPAC'12*, New Orleans, LA, USA, May 2012, paper MOYAP01, pp. 6–10, ISBN 978-3-95450-115-1.

[33] H. Takei *et al.*, "Estimation of acceptable beam-trip frequencies of accelerators for accelerator-driven systems and comparison with existing performance data", *J. Nucl. Sci. Techol.*, vol. 49, p. 384, Sep. 2012, doi:10.1088/00223131.2012.669239.

[34] J.-L. Biarrotte, Reliability and fault tolerance in the European ADS project, CERN Accelerator School: Course on High Power Hadron Machines, 24 May - 2 Jun 2011, Bilbao, Spain, 2013, doi:10.5170/CERN-2013-001.481.

[35] B. Yee-Rendon, "Overview of ADS Projects in the World", in *Proc. LINAC'22*, Liverpool, UK, Aug.-Sep. 2022, pp. 310–313, doi:10.18429/JACoW-LINAC2022-TU2AA01.

[36] Y. He *et al.*, "Development of Accelerator Driven Advanced Nuclear Energy and Nuclear Fuel Recycling", in *Proc. IPAC'19*, Melbourne, Australia, May 2019, pp. 4389–4393 doi:10.18429/JACoW-IPAC2019-TUYPLS2.

[37] H. Podlech *et al.*, "The MYRRHA Project", in *Proc. NAPAC'19*, Lansing, MI, USA, Sep. 2019, pp. 945–950, doi:10.18429/JACoW-NAPAC2019-THZBA2

[38] T. Sugawara *et al.*, "Research and Development Activities for Accelerator-Driven System in Jaea", *Prog. Nucl. Energy*, vol. 106, p. 27, Feb. 2018, doi:10.1016/j.pnucene.2018.02.007.

[39] J. S. Chai, "A Status and Prospect of Thorium-Based ADS in Korea", presented at the *Int. Thorium Energy Conf (ThEC13)*, Geneve, Switzerland, Oct. 2013, pp. 305–310, doi:10.1007/978-3-319-26542-1_45.

[40] S. Formin, "Accelerator-driven sub-critical system (ADS), Neutron source NSC KIPT", presented at the LIA workshop, Orsay, France, Oct. 2020, LIAWorkshop.

[41] Raja Rammanna Center for Advanced Technology, RRCATADS.

[42] S. F. Sidorkin *et al.*, "The ADS-Troitsk project", presented at the *Status of Accelerator Driven Systems Research and Technology Development workshop*, Geneve, Switzerland, Feb. 2017, Troitsk-ADSWS2017.

[43] R. P. Johnson, R. J. Abrams, M. A. Cummings, J. D. Lobo, M. Popovic, and T. J. Roberts, "Mu*STAR: A Modular Accelerator-Driven Subcritical Reactor Design", in *Proc. IPAC'19*, Melbourne, Australia, May 2019, pp. 3555–3557, doi:10.18429/JACoW-IPAC2019-THPMP048.

[44] M. Losasso, "CYCLADS, an EU FET proposal for high power cyclotron conceptual design", presented at the *Status of Accelerator Driven Systems Research and Technology Development workshop*, Geneve, Switzerland, Feb. 2017, Losasso-ADSWS2017.

[45] A . Billebaud *et al.*, The GUINEVERE Project for Accelerator Driven System Physics, Proc. of the Global 2009 conference, Paris, France, 2009, in2p3-00305892.

[46] M. A. Baylac *et al.*, "Operation Of The Versatile Accelerator Driving the Low Power ADS GUINEVERE at SCKCEN", in *Proc. LINAC'14*, Geneva, Switzerland, Aug.-Sep. 2014, paper TUPP100, pp. 659–661, isbn 978-3-95-450142-7.

[47] J.L. Lecouey,*et al.*, Estimate of the reactivity of the VENUS-F subcritical configuration using a Monte Carlo MSM method, Annals of Nuclear Energy, Volume 83, 2015, Pages 65-75, ISSN 0306-4549, doi:10.1016/j.anucene.2015.04.010.

[48] N. Marie, *et al.*, Reactivity monitoring of the accelerator driven VENUS-F subcritical reactor with the "current-to-flux" method, Annals of Nuclear Energy, Volume 128, 2019, Pages 12-23, ISSN 0306-4549, doi:10.1016/j.anucene.2018.12.033.

[49] A. Billebaud, *et al.*, Extended MSM Method to estimate reactivity of a sub-critical core driven by an accelerator based neutron source, EPJ Web Conf., Volume 247, 2021, doi:10.1051/epjconf/202124708005.

[50] A. Bailly, Mesure de la réactivité d'un réacteur sous critique à neutrons rapides, Normandie Université, Phd Thesis, 2022, tel-04032534.

[51] D. Vandeplassche *et al.*, "Integrated Prototyping in View of the 100 MeV Linac for Myrrha Phase 1", in *Proc. IPAC'18*, Vancouver, Canada, Apr.-May 2018, pp. 661–664, doi:10.18429/JACoW-IPAC2018-TUPAF003

[52] U. Dorda and A. Fabich, "Implementation status of MYRRHA phase 1 (MINERVA)", presented at the IPAC'23, Venice, Italy, May 2023, pp. 2617–2620, doi:10.18429/JACoW-IPAC2023-WEOGB3.

[53] A. Gatera *et al.*, "Minerva (MYRRHA Phase 1) RFQ Beam Commissioning", in *Proc. IPAC'21*, Campinas, Brazil, May 2021, pp. 675–678. doi:10.18429/JACoW-IPAC2021-MOPAB205.

[54] A. Gatera, J. Belmans, Dr. Ben Abdillah, F. Bouly, S. Boussa, F. Davin, *et al.*, "MYRRHA-MINERVA Injector Status and Commissioning", in *Proc. HB'21*, Batavia, IL, USA, Oct. 2021, pp. 186–190. doi:10.18429/JACoW-HB2021-WEBC3.

[55] F. Bouly *et al.*, "Superconducting LINAC Design Upgrade in View of the 100 MeV MYRRHA Phase I", in *Proc. IPAC'19*, Melbourne, Australia, May 2019, pp. 837–840. doi:10.18429/JACoW-IPAC2019-MOPTS003.

[56] Z. J. Wang *et al.*, "The Status of CiADS Superconducting LINAC", in *Proc. IPAC'19*, Melbourne, Australia, May 2019, pp. 994–997, doi:10.18429/JACoW-IPAC2019-MOPTS059.

[57] S.H. Liu *et al.*, "High Availability Oriented Physics design for CiADS Proton Linac", in *Proc. HB2023*, CERN, Switzerland, oct. 2023, TUC2I1.

[58] J. Tamura *et al.*, "Current Status of the Spoke Cavity Prototyping for the JAEA–ADS Linac", in *Proc. LINAC'22*, Liverpool, UK, Aug.-Sep. 2022, pp. 180–183. doi:10.18429/JACoW-LINAC2022-MOPOGE14.

[59] B. Yee-Rendon *et al.*, "Design and beam dynamic studies of a 30-MW superconducting linac for an accelerator-driven subcritical system", *Phys. Rev. Accel. Beams*, vol. 24, p. 120101, Dec. 2021, doi:10.1103/PhysRevAccelBeams.24.120101.

[60] B. Yee-Rendon *et al.*, "Beam dynamics studies for fast beam trip recovery of the Japan Atomic Energy Agency accelerator-driven subcritical system", *Phys. Rev. Accel. Beams*, vol. 25, p. 080101, Aug. 2021, doi:10.1103/PhysRevAccelBeams.25.080101.

[61] A. Placais, F. Bouly, and B. Yee-Rendon, "Development of a Tool for Cavity Failure Compensation in Superconducting Linacs: Progress and Comparative Study", presented at the IPAC'23, Venice, Italy, May 2023, paper THPA060, doi:10.18429/JaCoW-IPAC2023-THPA060.

[62] A. P. Shishlo and C. C. Peters, "Fully Automated Tuning and Recover of a High Power SCL", in *Proc. LINAC'22*, Liverpool, UK, Aug.-Sep. 2022, pp. 884–888, doi:10.18429/JACoW-LINAC2022-FR1AA06.

[63] F. Bouly, Etude d'un module accélérateur supraconducteur et de ses systèmes de régulation pour le projet MYRRHA, PhD Thesis, Université Paris Sud - Paris XI, 2011, tel-00660392.

[64] A. Placais and F. Bouly, "Cavity failure compensation strategies in superconducting linacs", in *Proc. LINAC'22*, Liverpool, UK, Aug.-Sep. 2022, pp. 552–555, doi:10.18429/JACoW-LINAC2022-TUPORI04.

[65] F. Bouly, J.-L. Biarrotte, and D. Uriot, "Fault Tolerance and Consequences in the MYRRHA Superconducting Linac", in *Proc. LINAC'14*, Geneva, Switzerland, Aug.-Sep. 2014, pp. 297–299 isbn 978-3-95-450142-7.

[66] J.-B. Clavel, Etude de systèmes et scénarios électronucléaires double strate de transmutation des actinides mineurs en ADS, Ecole des Mines de Nantes, 2012, tel-00789327.